

4) complement one another, except that STM makes very small particles (<1 nm) visible, which is not possible by TEM.

Wiesner *et al.* have postulated stabilizing electrostatic interaction between cetyltrimethylammonium ions and Ag surfaces (5). Assuming this general model and placing the H atoms of the α -methylene groups of the $^+NR_4$ ions at the outer surface of the metal core (Fig. 5), it is possible to calculate approximate values of S with standard MM2 force field calculations. The agreement between calculated and experimental values is excellent (Table 2). Thus, a monomolecular protective coat is involved. The results demonstrate that STM is a suitable tool for the visualization of surfactant layers on metal colloids and that the combination STM and high-resolution TEM leads to valuable information regarding the approximate geometric relation between the metal core and the stabilizing mantle. It is likely that the method of combined STM-TEM is not restricted to our materials.

The question remains how the results can be explained in terms of the STM imaging process. The STM images clearly show that the tip is withdrawn from the surface when it reaches a surfactant-covered metal cluster. The feedback mechanism of the STM holds the conductance between tip and sample at a constant value. Thus, the motion of the tip is along a line of constant tunnel resistance. Because the particles are imaged correctly regarding their size, the transfer of electrons through the surfactant layer must be fast and not dependent on the length of the carbon chain of the surfactant. The physical reason for this surprising result is not yet clear and has to be investigated further.

REFERENCES AND NOTES

- G. Schmid, *Clusters and Colloids* (VCH, Weinheim, Germany, 1994); H. Weller, *Angew. Chem.* **105**, 43 (1993) [*Angew. Chem. Int. Ed. Engl.* **32**, 41 (1993)]; S. C. Davis and K. J. Klabunde, *Chem. Rev.* **82**, 153 (1982); L. N. Lewis, *ibid.* **93**, 2693 (1993); B. C. Gates, L. Gucci, H. Knözinger, *Metal Clusters in Catalysis* (Elsevier, Amsterdam, 1986).
- J. S. Bradley, J. M. Millar, E. W. Hill, *J. Am. Chem. Soc.* **113**, 4016 (1991).
- G. Schmid, B. Morun, J.-O. Malm, *Angew. Chem. Lett.* **101**, 772 (1989) [*Angew. Chem. Int. Ed. Engl.* **28**, 778 (1989)]; M. N. Vargaftik, V. P. Zagorodnikov, I. P. Stolarov, I. I. Moiseev, *J. Mol. Catal.* **53**, 315 (1989).
- J. Kiwi and M. Grätzel, *J. Am. Chem. Soc.* **101**, 7214 (1979); Y. Sasson, A. Zoran, J. Blum, *J. Mol. Catal.* **11**, 293 (1981); M. Boutonnet, J. Kizling, R. Touroude, G. Maire, P. Stenius, *Appl. Catal.* **20**, 163 (1986); N. Tushima, T. Takahashi, G. Hirai, *Chem. Lett.* **1985**, 1245 (1985); K. Meguro, M. Torizuka, K. Esumi, *Bull. Chem. Soc. Jpn.* **61**, 341 (1988); N. Satoh and K. Kimura, *ibid.* **62**, 1758 (1989); H. Bönemann *et al.*, *Angew. Chem.* **103**, 1344 (1991) [*Angew. Chem. Int. Ed. Engl.* **30**, 1312 (1991)]; N. Tushima and T. Takahashi, *Bull. Chem. Soc. Jpn.* **65**, 400 (1992).
- J. Wiesner, A. Wokaun, H. Hoffmann, *Prog. Colloid Polym. Sci.* **76**, 271 (1988).
- G. Schmid and co-workers have studied a $P(p-C_6H_4SO_3Na)_2$ -protected gold colloid on a graphite surface by TEM [G. Schmid, *Chem. Rev.* **92**, 1709 (1992)].
- G. Binnig, H. Rohrer, C. Gerber, E. Weibel, *Appl. Phys. Lett.* **40**, 178 (1982); J. Frommer, *Angew. Chem.* **104**, 1325 (1992) [*Angew. Chem. Int. Ed. Engl.* **31**, 1298 (1992)].
- H. A. Wierenga *et al.*, *Adv. Mater.* **2**, 482 (1990); L. E. C. van de Leemput *et al.*, *J. Vac. Sci. Technol. B* **9**, 814 (1991).
- M. T. Reetz and W. Helbig, *J. Am. Chem. Soc.* **116**, 7401 (1994).
- K. Besocke, *Surf. Sci.* **181**, 145 (1987).

14 July 1994; accepted 6 October 1994

The Structure of Confined Oxygen in Silica Xerogels

B. S. Schirato,* M. P. Fang, P. E. Sokol,† S. Komarneni

The microscopic structure of oxygen confined in silica xerogels has been studied as a function of temperature. In large pores, a crystalline solid forms with a structure consistent with that of the bulk. The size of the crystallites is much larger than the pore size, indicating that cooperative effects among pores are important in freezing. As the pore size is decreased, a crossover occurs where solidification results in an amorphous phase in the pores. The resulting amorphous phase is solid but is less ordered than the liquid phase.

The confinement of liquids in restricted geometries leads to many new and interesting features (1). The interactions between molecules and surfaces in interconnected, random confining pores lead to many effects that are of fundamental interest. These effects are also of practical importance in areas such as interfacial adhesion, lubrication, rheology, and tribology.

Previous studies of freezing in porous media have shown significant deviations from bulk freezing (2–5), such as a depression of the freezing temperature and a large hysteresis between cooling and warming. The dynamical properties of the supercooled liquid are also different from those of conventional bulk liquids (2, 6). Recent computer simulations of freezing in confined geometries (7, 8) have resulted in enhanced, rather than suppressed, freezing temperatures. These simulations have also revealed structures different from the bulk that have been observed experimentally in some systems (8).

In this report, we present measurements of the static structure factor $S(Q)$ of oxygen confined in silica xerogels. The microscopic structure of the liquid or solid in the pores, which is reflected in $S(Q)$, is fundamental to obtaining an understanding of the effects of confinement, randomness, and geometrical interconnection on the properties of condensed phases in the pores. Xerogels (9) are porous materials with pore sizes ranging from 10 to 500 Å formed by the gelation

and compaction of silica solutions. They provide a convenient and well-characterized confining medium, and oxygen provides an interesting system for structural studies because it possesses both liquid-solid and solid-solid phase transitions (10), its structure is well known (11–13), and several previous studies of the behavior of oxygen adsorbed in xerogels exist (2, 8, 14). In addition, oxygen is weakly interacting, with respect to the xerogel glass, so that structural changes in the confining material do not occur.

We find that a crystalline solid forms in large pores with a structure consistent with that of the bulk system. The crystallite size of the solid in the pores is much larger than the pore size, indicating that freezing is a cooperative process involving interconnected pores. In small pores, unusual behavior is observed at the liquid-solid transition where solidification results in an amorphous solid phase that is less ordered than the liquid phase.

The xerogels were synthesized in a closed system by mixing 10 ml of tetramethylorthosilicate (TMOS) with 6 ml of various concentrations of HF and NaF with a H_2O /TMOS ratio of 4.96. No alcohol was added. Xerogels with pore diameters of 35, 45, and 60 Å were prepared with 0.1 M HF, 0.2 M HF, and 0.1 M NaF, respectively. The mixed solutions were stirred in airtight containers until gelation occurred. After gelation, gels were left in their respective bottles for about 12 hours before drying at 60° to 65°C for 2 days, which was followed by further drying at 200°C for 4 hours to obtain xerogels. The three gels were then characterized by water and nitrogen adsorption isotherms.

The neutron diffraction measurements were carried out with the Electron Volt

B. S. Schirato, M. P. Fang, P. E. Sokol, Department of Physics, Pennsylvania State University, University Park, PA 16802, USA.

S. Komarneni, Materials Research Laboratory, Pennsylvania State University, University Park, PA 16802, USA.

*Present address: Department of Physics, Cornell University, Clark Hall, Ithaca, NY 14853, USA.

†To whom correspondence should be addressed.

Spectrometer at the Intense Pulsed Neutron Source, Argonne National Laboratory. The gels were contained in a vanadium container attached to a closed-cycle refrigerator. The pores were slightly underfilled with oxygen (95% of full pore capacity) to prevent the formation of bulk solid. The results were converted to $S(Q)$ by standard techniques (15). The scattering from the oxygen alone was obtained by subtracting the signal of the cell containing the xerogel without oxygen adsorbed.

Figure 1 shows $S(Q)$ for oxygen confined in the 60 Å diameter pores at different temperatures. The scattering at 60 K, well above the bulk triple point of 54.4 K, exhibits a typical liquid structure with a broad maxima arising from the short-range correlations in the liquid. The scattering is identical to the bulk liquid (16) at the same temperature, which was also measured for comparison.

Supercooling of the liquid-solid transition in small pores stabilizes the liquid phase well below the bulk triple point. The scattering at 52 K, well below the bulk triple point of 54.4 K, still exhibits the $S(Q)$ characteristic of the liquid. The $S(Q)$ profile changes little in this temperature range, indicating that the structure of the liquid in the pores, even in the supercooled regime, is quite ordinary. Dynamical experiments (6), in contrast, have revealed quite different behavior for the supercooled liquid.

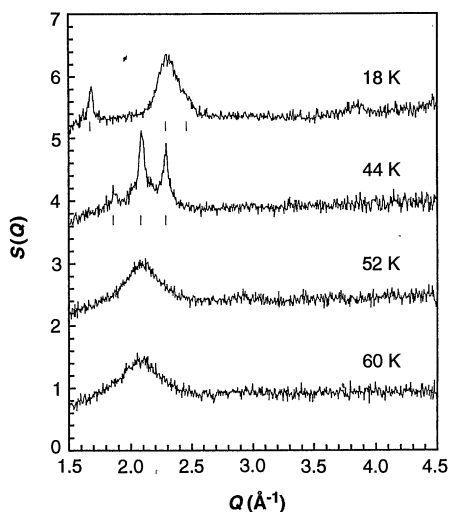


Fig. 1. The scattering from oxygen adsorbed in a xerogel with pores 60 Å in diameter. The scattering from the empty xerogel has been subtracted. The scattering is shown at temperatures of 60, 52, 44, and 18 K. The measurements correspond to the bulk liquid, supercooled liquid, γ , and β phases, respectively. The scattering for 52, 44, and 18 K have been offset for clarity. The solid lines beneath the scattering for the γ and β phases are the expected locations of diffraction peaks for the bulk structures. The peaks in the figure are the only peaks observed for values of Q up to 15 \AA^{-1} .

The liquid-solid transition of the oxygen in the pores is marked by the appearance of diffraction peaks, which are a clear indication of long-range translational correlations and solidification. The peaks appear over a very narrow temperature range (~ 1 K) at 50 K, well below the bulk liquid-solid transition. The structure of the solid phase in the pores cannot be directly determined from the diffraction data because the higher order peaks needed for a structural determination are missing, presumably damped as a result of the disorder introduced into the solid by the random surroundings (17). However, a comparison of the observed peaks with those expected for the bulk γ phase (13) shows that the observed peaks are consistent with the bulk structure. Thus, it appears that the crystalline structure of the oxygen in the pores is the same as that of the bulk system.

A second transition marked by a change in the location and shape of the diffraction peaks occurs at a temperature of 44 K. This transition corresponds to the γ - β transition in the bulk (11) where orientational ordering sets in. Once again, the transition temperature is below the bulk value, illustrating that supercooling is also present for first-order solid-solid transitions (2). The location of the peaks is consistent with the bulk β phase (11) when the effects of line broadening are taken into account (18). No further transitions were observed to the lowest temperature studied (18 K). In particular, the α - β transition, which occurs at 23.9 K in the bulk, was not observed. Thus, either the transition is suppressed by more than 6 K, which is larger than the observed suppression of the liquid- γ and γ - β transitions, or the confining media suppresses this phase.

The diffraction peaks in both the γ and β phases are significantly broader than the instrumental resolution because of factors such as the finite crystallite size and strains

(18). An analysis of the peak widths indicates that both solid phases are strained, with the lower temperature phase exhibiting increased strains. Furthermore, the crystallite size, based on the estimated peak width at $Q = 0$, is on the order of 700 to 1000 Å, much larger than the average pore diameter of 60 Å. The crystalline regions that form in the pore space must extend between pores because no single pore is large enough to support crystallites of this size. This implies that solidification occurs by nucleation in a single pore followed by growth of the crystalline region through adjoining pores.

An amorphous, or "liquid-like", component is also present in the scattering from the solid phase, which is presumably the result of molecules strongly bound to the random surface of the pore walls. The amorphous component should also be present in the liquid; however, its presence is probably masked by the amorphous-like scattering of the liquid.

We have examined the effect of pore size using xerogels with pore sizes of 35 and 45 Å. The 45 Å sample exhibits results similar to the larger pore sample. Crystalline phases with long-range order and the same structure as the bulk are observed. The transition temperatures to these phases are consistent with previous measurements (2). The amorphous component is more prominent in the 45 Å pores, as compared to the 60 Å pores, presumably because of the larger surface to volume ratio of the smaller pore sample.

The smallest pore samples studied, with a pore size of 35 Å, exhibit unusual behavior (Fig. 2). At high temperatures, the structure of the liquid in the pores is the same as that of the bulk liquid, just as in the larger pores. However, upon cooling no diffraction peaks, which are indicative of a crystalline phase, are observed down to the minimum temperature studied (20 K). There is, however, a definite change in the observed scattering, indicating that

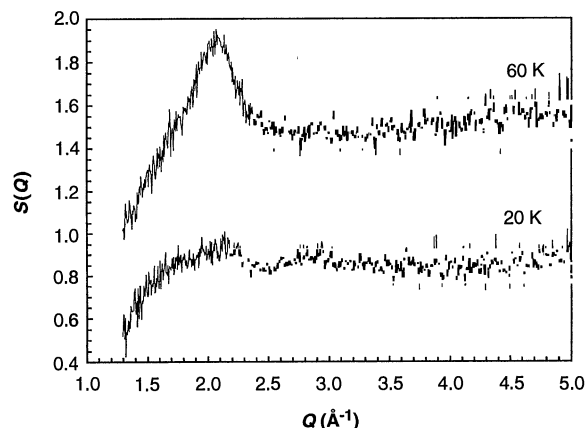


Fig. 2. The scattering from the oxygen adsorbed in a silica xerogel with pore size 35 Å at temperatures of 20 and 60 K. The silica scattering has been removed, and the scattering for 60 K has been shifted for clarity.

the microscopic structure of the adsorbed O_2 has changed. The lack of diffraction peaks indicates that this is a liquid-glass, rather than a liquid-crystalline solid transition such as occurs in larger pores.

The scattering measurements indicate that an amorphous solid phase is formed in the small pores at low temperature. The structure of this solid phase is quite unusual. The local ordering in the solid, as reflected by the variations in $S(Q)$, is much less than that in the liquid phase. This is quite different from other amorphous systems, such as glasses, where the local ordering is similar to that of the liquid and the structure in $S(Q)$ usually sharpens slightly with respect to the liquid when the glass forms, reflecting the increased atomic correlations in the glass phase (19). However, our results indicate that the atomic correlations of the solid phase in the pores are significantly smaller than those of the liquid. In fact, the almost complete disappearance of structure in $S(Q)$ upon cooling indicates that correlations between atoms in the solid are extremely small. Such a transition where the solid exhibits much less order than the liquid is, to our knowledge, unique.

It is important to emphasize that the decrease in structure of $S(Q)$ upon cooling is not caused by the migration of material out of the pore space. The total scattering at large Q , which is proportional to the amount of material in the pores, does not change significantly upon cooling. Thus, the oxygen in the pores does not migrate to other regions out of the neutron beam, and our results are representative of the freezing of oxygen in these small pores.

The origin of this solid phase is not clear at present. It must, however, be related to the large surface to volume ratio in the small-pore samples. Each oxygen molecule adsorbed in the pores feels a significant interaction with the walls because of the strong substrate-adsorbate interaction. This leads to a frustration in which the oxygen molecules cannot minimize energy with respect to both neighboring molecules and the surrounding random porous medium at the same time. Thus, the solid phase that is formed is a compromise between these competing influences and exhibits almost no correlations between the oxygen molecules in the pores.

A simple physical interpretation emerges from these results. Near the walls, the molecules are strongly influenced by the complex amorphous structure of the walls. They accommodate this structure as best they can, leading to an added amorphous component in the scattering observed for the large-pore samples. There is then a healing length away from the walls where the disorder induced by the walls is annealed out. For large pores, this

annealing process is complete, and a crystalline phase appears in the center of the pores. For smaller pores, the disorder cannot anneal out, and a unique glass phase is formed.

REFERENCES AND NOTES

1. J. Klafter and J. M. Drake, *Molecular Dynamics in Restricted Geometries* (Wiley, New York, 1989).
2. J. Warnock, D. D. Awschalom, M. W. Shafer, *Phys. Rev. Lett.* **57**, 1753 (1986).
3. C. L. Jackson and G. B. McKenna, *Rubber Chem. Technol.* **64**, 760 (1990).
4. R. H. Torii, H. J. Maris, G. M. Seidel, *Phys. Rev. B* **41**, 7167 (1990).
5. E. Molz, A. P. Y. Wong, M. H. W. Chan, *ibid.* **48**, 5741 (1993).
6. M. B. Ritter, D. D. Awschalom, M. W. Shafer, *Phys. Rev. Lett.* **61**, 966 (1988).
7. W.-J. Ma, J. R. Banavar, J. Koplik, *J. Chem. Phys.* **97**, 485 (1992).
8. P. E. Sokol *et al.*, *Appl. Phys. Lett.* **61**, 777 (1992).
9. R. K. Iler, *The Chemistry of Silica* (Wiley, New York, 1979).
10. J. W. Stewart, *J. Phys. Chem. Solids* **12**, 122 (1959).
11. M. F. Collins, *Proc. Phys. Soc. London* **89**, 415 (1966).

12. R. J. Meier, R. B. Helmholtz, *Phys. Rev. B* **29**, 1387 (1984).
13. T. H. Jordan, W. E. Streib, H. Warren, *Acta Crystallogr.* **17**, 777 (1964).
14. D. D. Awschalom, J. Warnock, M. W. Shafer, *Phys. Rev. Lett.* **57**, 1607 (1986).
15. P. A. Egelstaff, in *Methods of Experimental Physics*, D. L. Price and K. Skold, Eds. (Academic Press, New York, 1987), vol. 23, part B, pp. 405–468.
16. K. S. Pederson, F. Y. Hansen, K. Carperio, *J. Chem. Phys.* **70**, 1051 (1979).
17. W. Schmatz, in (15), pp. 85–126.
18. H. P. Klug and H. P. Alexander, *X-ray Diffraction Procedures for Polycrystalline and Amorphous Materials* (Wiley, New York, 1974).
19. S. Kenji, in (15), pp. 243–300.
20. This work was supported by National Science Foundation grant DMR-91-23469, Petroleum Research Fund contract 26046-AC7E, Gas Research Institute contract 50872601473, and Office of Basic Energy Science—Division of Materials Research support of the Intense Pulsed Neutron Source at Argonne National Laboratory under Department of Energy grant W-31-109-ENG-38. B.S.S. acknowledges the support of the Division of Educational Programs at Argonne National Laboratory.

5 May 1994; accepted 11 October 1994

Host Range of a Plant Pathogenic Fungus Determined by a Saponin Detoxifying Enzyme

P. Bowyer, B. R. Clarke, P. Lunness, M. J. Daniels, A. E. Osbourn*

Antifungal saponins occur in many plant species and may provide a preformed chemical barrier to attack by phytopathogenic fungi. Some fungal pathogens can enzymatically detoxify host plant saponins, which suggests that saponin detoxification may determine the host range of these fungi. A gene encoding a saponin detoxifying enzyme was cloned from the cereal-infecting fungus *Gaeumannomyces graminis*. Fungal mutants generated by targeted gene disruption were no longer able to infect the saponin-containing host oats but retained full pathogenicity to wheat (which does not contain saponins). Thus, the ability of a phytopathogenic fungus to detoxify a plant saponin can determine its host range.

Plant disease resistance may be mediated by active responses, triggered after pathogen attack, and by preformed substances that serve as plant protectants. Saponins (glycosylated steroidal or triterpenoid compounds) are common plant secondary metabolites occurring in over 100 families, and because many saponins have pronounced antifungal properties, it is possible that they act as preformed determinants of resistance to attack by fungi (1–4). The toxic effects of saponins are attributed to their ability to form complexes with membrane sterols, resulting in loss of membrane integrity (5, 6). Some pathogenic fungi have intrinsic resistance to the membraneolytic action of saponins because of their membrane composition (4, 7), whereas others produce enzymes that specifically detoxify particular plant saponins (4, 8–14). These enzyme activities have been associat-

ed with the ability to attack certain plants. This implies that, at least for some interactions, “saponin-saponinase” combinations may dictate the outcome of attempted infection of plants by fungi.

A paradigm case is the interaction between the root-infecting fungus *Gaeumannomyces graminis* and cereals. Isolates of *G. graminis* that infect oats (*G. graminis* var. *avenae*, or *Gga*) are relatively insensitive to the oat root saponin avenacin A-1, whereas *G. graminis* var. *tritici* (*Ggt*) isolates are unable to infect most oat species and are sensitive to avenacin A-1 (8–10). Both *Gga* and *Ggt* are pathogenic to the non-saponin-containing host, wheat. Avenacin A-1 is localized in the epidermal cells of the oat root (15) and hence may constitute one of the first barriers to infection by sensitive fungi such as *Ggt*. The one oat species that lacks avenacin A-1, *Avena longiglumis*, is susceptible to infection by *Ggt* (15). These observations are consistent with a role for avenacin A-1 as a determinant of resistance

The Sainsbury Laboratory, John Innes Centre, Norwich Research Park, Norwich NR4 7UH, UK.

*To whom correspondence should be addressed.